

---

# Control-Oriented Model-Based Reinforcement Learning with Implicit Differentiation

---

Evgenii Nikishin<sup>1</sup> Romina Abachi<sup>2</sup> Rishabh Agarwal<sup>1,3</sup> Pierre-Luc Bacon<sup>1,4</sup>

<sup>1</sup>Mila, Université de Montréal, <sup>2</sup>Vector Institute, University of Toronto  
<sup>3</sup>Google Research, Brain Team, <sup>4</sup>Facebook CIFAR AI Chair

## Abstract

The shortcomings of maximum likelihood estimation in the context of model-based reinforcement learning have been highlighted by an increasing number of papers. When the model class is misspecified or has a limited representational capacity, model parameters with high likelihood might not necessarily result in high performance of the agent on a downstream control task. To alleviate this problem, we propose an end-to-end approach for model learning which directly optimizes the expected returns using implicit differentiation. We treat a value function that satisfies the Bellman optimality operator induced by the model as an implicit function of model parameters and show how to differentiate the function. We provide theoretical and empirical evidence highlighting the benefits of our approach in the model misspecification regime compared to likelihood-based methods.

## 1 Introduction

The conceptual separation between model learning and policy optimization is the basis for much of the work on model-based reinforcement learning (MBRL) [28, 73, 53, 12, 17, 33, 40, 44]. A standard MBRL agent first estimates the transition parameters and the reward function of a Markov Decision Process and then uses the approximate model for planning [77, 49, 56, 27, 13, 37, 57, 69]. If the estimated model perfectly captures the actual system, the resulting policies are not affected by the model approximation error. However, if the model is imperfect, the inaccuracies can lead to nuanced effects on the policy performance [2, 57]. Several works [71, 43, 50] have pointed out on *the objective mismatch* in MBRL and demonstrated that optimization of model likelihood might be unrelated to optimization of the returns achieved by the agent that uses the model. For example, accurately predicting individual pixels of the next state [44] might be neither easy nor necessary for decision making. Motivated by these observations, our paper studies control-oriented model learning that takes into account how the model is used by the agent.

While much of the work in control-oriented model learning has focused on robust or uncertainty-based methods [55, 61, 39, 82, 83], we propose an algorithm for learning a model that directly optimizes the expected return using implicit differentiation [16, 29]. Specifically, we assume that there exists *an implicit function* that takes the model as input and outputs a value function that is a fixed point of the Bellman optimality operator [20] induced by the model. We then calculate the derivatives of the optimal value function with respect to the model parameters using the implicit function theorem (IFT), allowing us to form a differentiable computational graph from model parameters to the sum of rewards. In reference to [67, 72, 7], we call our control-oriented method *optimal model design* (OMD).

Our contributions can be summarized as follows:

- We propose OMD, an end-to-end MBRL method that optimizes expected returns directly.
- We characterize the set of OMD models in the tabular case and derive an approximation bound on the optimal value function that is tighter than the likelihood-based bound.

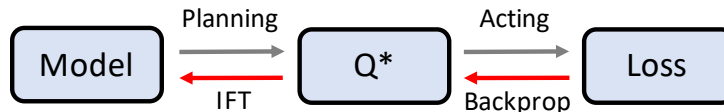


Figure 1: Illustration of the *Optimal Model Design* approach: we treat the optimal Q-function as an implicit function of the model and calculate the gradient with respect to model parameters via the implicit function theorem as described in Section 4.1.

- We propose a series of approximations to scale our approach to non-tabular environments.
- We demonstrate that OMD outperforms likelihood-based MBRL agents under the model misspecification in both tabular and non-tabular settings. This finding suggests that our method should be preferred when we cannot approximate the true model accurately.
- We empirically demonstrate that models obtained by OMD can have lower likelihood than a random model yet generate useful targets for updating the value function. This finding suggests that likelihood optimization might be an unnecessary step for MBRL.

## 2 Related work

**Learning control-oriented models.** Earlier work in optimal control and econometrics [71, 67] studied the relation between the model approximation error and the control performance and noted that true parameter identification could be suboptimal when the model class is limited. Joseph et al. [43] were one of the first to address the objective mismatch [50] and proposed an algorithm for training models that maximize the expected returns using zero-order optimization.

Several papers have proposed model learning approaches that optimize other return-aware objectives. Farahmand et al. [23] train a model to minimize the difference between values of the real next states and the next states predicted by the dynamics. Abachi et al. [1] use the norm of the difference between policy gradients as the model objective. D’Oro et al. [22] use a weighted maximum likelihood objective where the weights are chosen to minimize the difference between the true policy gradient and the policy gradient in the MDP induced by the model. Schrittwieser et al. [70] use tree search and train a model for image-based states by encoding them into a latent space and predicting a reward, a policy, and values without reconstructing the images.

The idea of differentiable planning has also been investigated. Amos et al. [4] learn a model via differentiating the Karush–Kuhn–Tucker conditions in the LQR setting [21]. Tamar et al. [76] uses a differentiable approximation of the value iteration algorithm to learn a planner. Amos and Yarats [3] optimize the parameters of a sampling distribution in Cross-Entropy Method [66] using a differentiable approximation of Top-K operation.

Several works have theoretically studied the control-oriented model learning. Ayoub et al. [5] derive regret bounds for models used to predict values. Grimm et al. [30] introduce the principle of value equivalence for MBRL defining two models to be equivalent if they induce the same Bellman operator.

Our work is closely related to the above papers but proposes to learn models by directly optimizing the sum of rewards in an end-to-end manner via gradient-based methods.

**Implicit function theorem.** Implicit differentiation has been applied for a variety of bi-level optimization problems. Lorraine et al. [54] treat weights of a neural network as an implicit function of hyperparameters and use IFT to optimize the hyperparameters. Rajeswaran et al. [64] study meta-learning and apply IFT to compute the outer loop gradient without the need to differentiate through the inner loop iterations. Instead of treating a neural network as a sequence of layers that transform an input, Bai et al. [8] propose an implicit layer that corresponds to an infinite depth neural network and find a fixed point of the layer via IFT. Our method also solves a bi-level problem: in the inner loop, we train an action-value function compatible with the model, while in the outer loop we update the model parameters towards maximizing the expected returns.

### 3 Preliminaries

Reinforcement Learning (RL) [74] methods follow the Markov Decision Process (MDP) formalism. An MDP is defined as  $\mathcal{M} = (\mathcal{S}, \mathcal{A}, \gamma, p, r, \rho_0)$ , where  $\mathcal{S}$  is a state space,  $\mathcal{A}$  is an action space,  $p(s'|s, a)$  is a transition probability distribution (often called *dynamics*),  $r(s, a)$  is a reward function,  $\gamma \in [0, 1]$  is a discount factor, and  $\rho_0(s)$  is an initial state distribution. The pair  $(p, r)$  is jointly called *the true model*. The goal of an agent is to learn a policy  $\pi(a|s)$  that maximizes the expected discounted sum of rewards  $J(\pi) = \mathbb{E}_\pi [\sum_{t=0}^{\infty} \gamma^t r(s_t, a_t)]$ . The performance of the agent following the policy  $\pi$  can also be quantified using the action value function  $Q^\pi(s, a) = \mathbb{E}_\pi [\sum_{t=0}^{\infty} \gamma^t r(s_t, a_t) | s_0 = s, a_0 = a]$ .

Model-based RL algorithms typically train a model  $(p_\theta, r_\theta)$  and use it for policy or value learning. Traditional methods based on Dyna [73] rely on maximum likelihood estimation (MLE) of model parameters  $\theta$ . For example, if the true model is assumed to be Gaussian with a parameterized mean and a fixed variance, maximizing the likelihood is equivalent to minimizing the mean squared error of the prediction, namely, to solving

$$\min_{\theta} \mathbb{E}_{s,a,s'} [\|f_\theta(s, a) - s'\|^2], \quad \min_{\theta} \mathbb{E}_{s,a,r} [(r_\theta(s, a) - r)^2]. \quad (1)$$

### 4 Optimal Model Design for Tabular MDPs

Consider a modification of the original RL problem statement, which was first proposed by Rust [67] and revisited by Bacon et al. [7]. In addition to maximizing the expected returns  $J$ , we introduce a constraint forcing the action value function  $Q$  to satisfy the Bellman equation induced by the model. The optimization problem becomes

$$\max_{Q, \theta} J(\pi_Q) \quad \text{s.t. } Q(s, a) = B^\theta Q(s, a) \quad \forall s \in \mathcal{S}, a \in \mathcal{A}. \quad (2)$$

$B^\theta$  is the soft Bellman optimality operator with respect to the model and  $\pi_Q$  is the softmax policy:

$$B^\theta Q(s, a) \triangleq r_\theta(s, a) + \gamma \mathbb{E}_{p_\theta(s'|s, a)} \log \sum_{a'} \exp Q(s', a'), \quad \pi_Q(a|s) = \frac{\exp Q(s, a)}{\sum_{a'} \exp Q(s, a')}. \quad (3)$$

We choose the soft Bellman operator with  $\log \sum_{a'} \exp Q(s', a')$  over the “hard” version with  $\max_{a'} Q(s', a')$  because of the differentiability of log-sum-exp. We also use a temperature  $\alpha$  in softmax and log-sum-exp but omit it from the expressions for simplicity. Note that finding a fixed point of the soft Bellman optimality operator corresponds to solving the MaxEnt RL formulation [84], but for a sufficiently small value of  $\alpha$ , the difference is negligible.<sup>1</sup>

Suppose there exists an *implicit* function  $\varphi(\theta) = Q^*$  that takes as input a model and outputs a Q-function that satisfies the constraint in (2). The sequence of transformations from the model parameters to the agent’s performance can be described then using the following graph:

$$\theta \xrightarrow{\varphi} Q^* \xrightarrow{\text{exp}} \pi_{Q^*} \xrightarrow{\text{act}} J. \quad (4)$$

In Section 4.1, we show how  $\frac{\partial \varphi(\theta)}{\partial \theta}$  can be calculated using the implicit function theorem (IFT). Since  $\frac{\partial J(\pi)}{\partial \pi}$  can be calculated using the policy gradient theorem [75], we can apply automatic differentiation to calculate the gradient with respect to  $\theta$ :

$$\frac{\partial J(\theta)}{\partial \theta} = \underbrace{\frac{\partial J(\pi)}{\partial \pi}}_{\text{PG}} \cdot \underbrace{\frac{\partial \pi(Q^*)}{\partial Q^*}}_{\text{softmax}} \cdot \underbrace{\frac{\partial \varphi(\theta)}{\partial \theta}}_{\text{IFT}}. \quad (5)$$

Given the expression for the gradient of  $J$  with respect to  $\theta$ , we use an appropriate optimization method to train the model. We call the approach *optimal model design* (OMD). Note that Dyna-based methods also train the Q-function to satisfy the constraint in (2) while using the likelihood as the objective for model parameters  $\theta$  [65]. In contrast, we train  $\theta$  to *directly optimize* the expected returns.

<sup>1</sup>More details about the soft Bellman operator and MaxEnt RL could be found in [51].

The optimization problem (2) suggests that OMD is a policy-based method [75]. However, we can turn it into a value-based approach [81] by replacing the objective  $J(\pi_Q)$  with the Bellman error:

$$\min_{Q, \theta} L^{\text{true}}(Q) \triangleq \sum_{s,a} (Q(s,a) - BQ(s,a))^2 \quad \text{s.t. } Q(s,a) = B^\theta Q(s,a) \quad \forall s \in \mathcal{S}, a \in \mathcal{A}, \quad (6)$$

where  $B$ , similarly to  $B^\theta$ , is the soft Bellman operator but induced by *the true reward  $r$  and dynamics  $p$* . We discuss the relation between the models obtained by solving problems (2) and (6) in Section 5.1.

While the constraint  $Q(s,a) = B^\theta Q(s,a)$  has to be satisfied for all state-action pairs limiting the approach to tabular MDPs, we show an extension to the function approximation case in Section 6.

#### 4.1 Implicit Differentiation

In this subsection, we state the implicit function theorem used to calculate  $\frac{\partial \varphi(\theta)}{\partial \theta}$ .

**Theorem 1.** (Cauchy, Implicit Function) *Let  $f : \Theta \times \mathcal{W} \rightarrow \mathcal{W}$  be a continuously differentiable function and  $(\tilde{\theta}, \tilde{w})$  be a point satisfying  $f(\tilde{\theta}, \tilde{w}) = \mathbf{0}$ . If the Jacobian  $\frac{\partial f(\tilde{\theta}, \tilde{w})}{\partial w}$  is invertible, then there exists an open set  $U \subseteq \Theta$  containing  $\tilde{\theta}$  and a unique continuously differentiable function  $\varphi$  such that  $\varphi(\tilde{\theta}) = \tilde{w}$  and  $f(\theta, \varphi(\theta)) = \mathbf{0}$  for all  $\theta \in U$ . Moreover,*

$$\frac{\partial \varphi(\theta)}{\partial \theta} = - \left( \frac{\partial f(\theta, w^*)}{\partial w} \right)^{-1} \cdot \frac{\partial f(\theta, w^*)}{\partial \theta} \Big|_{w^* = \varphi(\theta)} \quad \forall \theta \in U. \quad (7)$$

We provide a proof in Appendix B. Note that (7) requires only a final point  $w^*$  satisfying the constraint and does not require knowledge about  $\varphi$  itself. Hence,  $\varphi$  can be any black-box function outputting  $w^*$ . The gradient of the scalar objective  $J$  or  $L^{\text{true}}$  is calculated using (7). To use backpropagation, we only need to define the product of a vector and  $\frac{\partial \varphi(\theta)}{\partial \theta}$ . We provide an implementation of a custom vector-Jacobian product for the implicit function  $\varphi$  in Appendix A allowing to use  $\varphi$  as a block in a differentiable computational graph.

#### 4.2 Benefits under Model Misspecification

In the previous subsection, we showed how to use implicit differentiation for training a model that aims to maximize the expected returns. In this subsection, we demonstrate that such a control-oriented model is preferable over a likelihood-based in the setting where the true model is not representable by a chosen parametric class.

Let  $r_\theta \in \mathbb{R}^{|\mathcal{S}| \times |\mathcal{A}|}$  and  $p_\theta(s'|s, a) \in \mathbb{R}^{|\mathcal{S}| \times |\mathcal{S}| \times |\mathcal{A}|}$  be a parametric model, where parameters in  $p_\theta$  denote the corresponding logits and each parameter in  $r_\theta$  is a reward for a state-action pair. We consider a set of parameters  $\{\theta : \|\theta\| \leq \kappa\}$  with the *bounded norm* and use  $\kappa$  as a measure of the model misspecification. By decreasing the bound of the norm of  $\theta$ , we get a more misspecified model class. To isolate the model learning aspect, we consider the exact RL setting without sampling. We take a 2 state, 2 action MDP shown in Figure 3 with a discount factor  $\gamma = 0.9$  and a uniform initial distribution  $\rho_0$ . For every  $\theta$ , a function  $\varphi$  outputs the corresponding  $Q^*$  via performing the fixed point iteration until convergence.  $Q^*$  is transformed into the policy  $\pi_{Q^*}$  via softmax with the temperature  $\alpha = 0.01$ . Given the policy  $\pi_{Q^*}$ , we calculate  $J$  in a closed form [74].

For OMD, we obtain the gradient of  $J$  with respect to  $\theta$  using the expression (5). We then apply the projected gradient ascent where after each step we make a projection on a space of bounded parameters via clipping  $\theta$  to  $\frac{\kappa}{\|\theta\|}\theta$  if  $\|\theta\| > \kappa$ . Finding an MLE solution corresponds to minimizing the average KL divergence

$$\overline{\text{D}}_{\text{KL}}(p||p_\theta) = \frac{1}{|\mathcal{S}| \cdot |\mathcal{A}|} \sum_{s,a,s'} p(s'|s,a) \log \frac{p(s'|s,a)}{p_\theta(s'|s,a)}$$

for optimizing  $p_\theta$  and minimizing the squared error for  $r_\theta$ . We similarly perform the projected gradient descent and call the agent MLE (despite having the exact setting without estimation).

The resulting  $J$  as a function of the norm bound  $\kappa$  is shown in Figure 2. When the true model is not representable by a chosen class, OMD learns a model that uses its representational capacity for

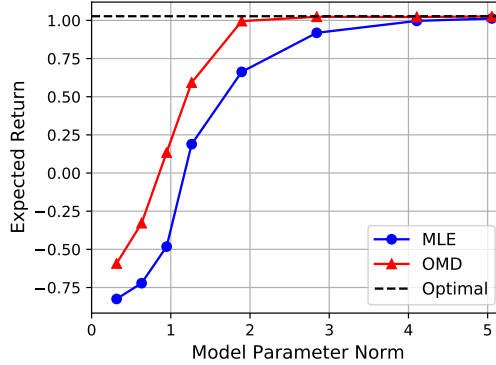


Figure 2: Expected returns for the tabular MDP under the model class misspecification. The OMD model optimizes the expected returns directly, while the MLE agent minimizes the KL divergence for model learning. OMD outperforms MLE when the model representational capacity is limited.

helping the agent to maximize the expected returns, while the MLE agent tries to predict the next states and rewards accurately while discarding the true objective function the agent seeks to optimize.

In MDPs with high-dimensional state spaces [11, 10] where the underlying dynamics are complex, having a model that will accurately predict the next observation might be expensive and unnecessary for decision making. Figure 2 reflects the problems an MLE-based model will face for such environments and provides evidence for using control-oriented models that leverage the available capacity of the model more effectively.

## 5 Theoretical Analysis

In the previous section, we have empirically demonstrated that OMD outperforms Dyna-style [73] MBRL agents when the model capacity is limited. This section characterizes the set of optimal solutions of OMD and compares the  $Q^*$  approximation bounds for OMD and MLE agents.

### 5.1 Optimal Solutions for OMD

We use the principle of value equivalence for MBRL [30] and argue that value equivalent models are optimal solutions to (2) and (6).

**Definition 1** (Optimal value equivalence). *Let  $Q^*$  be an optimal action-value function for the unconstrained RL problem. The models with parameters  $\theta$  and  $\theta'$  are  $Q^*$ -equivalent if*

$$B^\theta Q^*(s, a) = B^{\theta'} Q^*(s, a) \quad \forall s \in \mathcal{S}, a \in \mathcal{A}. \quad (8)$$

The definition is a slight modification of the value equivalence used in [30]: instead of requiring the Bellman operators to be equal for a set of value functions and policies, we require the equality for a chosen  $Q^*$  only. The subset of models that are  $Q^*$ -equivalent forms an *equivalence class*  $\Theta_{Q^*}$ .

**Proposition 1.** *If we let the soft Bellman operator (3) temperature  $\alpha \rightarrow 0$  and let  $\theta$  be any model parameters from the equivalence class  $\Theta_{Q^*}$ , then  $(Q^*, \theta)$  is a solution for (2) and (6).*

This property holds by construction. The optimal Q-function maximizes the objective in the true MDP. As the log-sum-exp temperature in (3) approaches 0, we recover the “hard” target in the Bellman optimality operator:

$$\lim_{\alpha \rightarrow 0} \alpha \log \sum_{a'} \exp \frac{1}{\alpha} Q(s', a') = \max_{a'} Q(s', a'). \quad (9)$$

Thus, if we set  $\theta$  to the true model,  $Q^*$  will satisfy the Bellman equation  $Q^*(s, a) = B^\theta Q^*(s, a)$ . But even though the true model belongs to the equivalence class  $\Theta_{Q^*}$ , it is *not identifiable*: all models from  $\Theta_{Q^*}$  are going to be indistinguishable for OMD. Seemingly undesirable at first glance, it allows OMD choosing *any* model that induces the same Bellman operator, which is beneficial under the model misspecification as shown in Section 4.2.

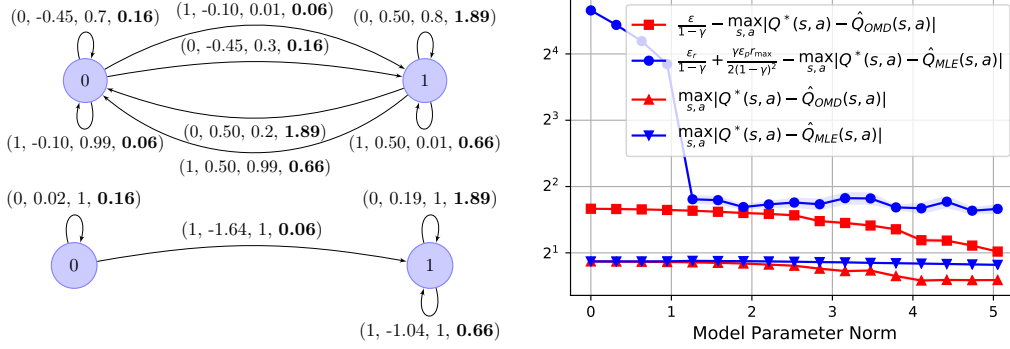


Figure 3: **Left:** Two different MDPs with the same optimal Q-function (a fixed point of the induced Bellman operator). Circles represent states, tuples are organized as (action, reward, transition probability, optimal Q value). Top: the original MDP taken from [18]. Bottom: an MDP with a trained OMD model. **Right:**  $Q^*$  approximation error and tightness of the error bounds under the model misspecification. Given a limited model representation capacity, OMD agent approximates  $Q^*$  more accurately and enjoys a tighter bound.

We provide an example of a model that is  $Q^*$ -equivalent with the true model in Figure 3. The model differs significantly, demonstrating that the equivalence class  $\Theta_{Q^*}$  consists of multiple elements. Moreover, the dynamics learned by OMD are deterministic, suggesting that OMD can choose a simpler model that will have the same  $Q^*$  as the true model. Drawing the connection to the prior work on state abstractions [52], the fact that MDPs have the same optimal action values indicates that the learned models can be seen as  $Q^*$ -irrelevant with respect to a state abstraction over  $S$ .

## 5.2 Approximation Bound

Our next result relates approximation errors for the optimal Q-functions under the OMD and MLE models. For simplicity, we analyze the setting with  $\alpha \rightarrow 0$  and the Bellman error (6) as the objective.

**Theorem 2.** ( $Q^*$  approximation error) *Let  $Q^*$  be the optimal action-value function for the true MDP. Let  $\hat{Q}_{\text{OMD}}$  and  $\hat{Q}_{\text{MLE}}$  be the fixed points of the Bellman optimality operators for approximate OMD and MLE models respectively. Then,*

- *If the MLE dynamics  $\hat{p}$  and reward  $\hat{r}$  have the bounded errors  $\max_{s,a} \|p(\cdot|s,a) - \hat{p}(\cdot|s,a)\|_1 = \epsilon_p$  and  $\max_{s,a} |r(s,a) - \hat{r}(s,a)| = \epsilon_r$ , and the reward function is bounded  $r(s,a) \in [0, r_{\max}] \forall s,a$ , we have*

$$\max_{s,a} \left| Q^*(s,a) - \hat{Q}_{\text{MLE}}(s,a) \right| \leq \frac{\epsilon_r}{1-\gamma} + \frac{\gamma\epsilon_p r_{\max}}{2(1-\gamma)^2};$$

- *If the Bellman optimality operator induced by the OMD model  $\hat{\theta}$  has the bounded error  $\max_{s,a} \left| B\hat{Q}_{\text{OMD}}(s,a) - B^{\hat{\theta}}\hat{Q}_{\text{OMD}}(s,a) \right| = \epsilon$ , we have*

$$\max_{s,a} \left| Q^*(s,a) - \hat{Q}_{\text{OMD}}(s,a) \right| \leq \frac{\epsilon}{1-\gamma}.$$

We prove the bounds in Appendix G using similar arguments as the proof of the simulation lemma [46]. The MLE bound has a  $\frac{1}{(1-\gamma)^2}$  term making the bound loose compared to the OMD bound with only the  $\frac{1}{1-\gamma}$  term. The bound suggests that OMD approximation error translates into a lower  $Q^*$  approximation error than for the MLE model. Figure 3 compares empirically the errors and the tightness of the bounds for a tabular MDP where  $Q^*$  can be computed exactly. The result provides evidence that OMD indeed achieves a lower  $Q^*$  approximation error compared to an agent that seeks to estimate  $p$  and  $r$  accurately. Motivated by the theoretical findings, the next section discusses a practical version of OMD.

---

**Algorithm 1** Model Based RL with Optimal Model Design

---

**Input:** Initial parameters  $w$  and  $\theta$ , empty replay buffer  $\mathcal{D}$ .

**repeat**

Set  $s$  to the current state, sample an action  $a$  using softmax over  $Q_w(s, a)$ .

Take the action  $a$ , observe  $r = r(s, a)$ ,  $s' \sim p(s'|s, a)$ , add  $(s, a, s', r)$  to  $\mathcal{D}$ .

**for**  $i = 1$  **to**  $K$  **do**

Sample  $(s, a)$  from  $\mathcal{D}$ , apply the model to get  $r = r_\theta(s, a)$ ,  $s' \sim p_\theta(s'|s, a)$ .

Update  $Q_w$  parameters  $w$  to minimize  $L(\theta, w)$ .

**end for**

Update model parameters  $\theta$  according to (13).

**until** the maximum number of interactions is reached

---

## 6 OMD with Function Approximation

Section 4 describes optimal model design, a non-likelihood-based method for learning models in tabular MDPs. In this section, we propose several approximations to make OMD practically applicable. We analyze the effect of the approximations and perform an ablation study in Appendix E.

**Q-network.** We use a neural network with parameters  $w$  to approximate the Q-values. The network is trained to minimize the Bellman error induced by the model  $\theta$ :

$$L(\theta, w) \triangleq \mathbb{E}_{s,a}[Q_w(s, a) - B^\theta Q_{\bar{w}}(s, a)]^2 \rightarrow \min_w, \quad (10)$$

where  $\bar{w}$  is a target copy of parameters  $w$  updated using exponential moving average, a standard practice to increase the stability of deep Q-learning [59]. We also use double Q-learning [35, 25] but omit it from the equations for simplicity. To estimate the expectation, we use a replay buffer [59].

**Constraint.** The constraint in (2) and (6) should be satisfied for all state-action pairs making it impractical for non-tabular MDPs. We introduce an alternative but similar constraint, the first-order optimality condition for minimizing the Bellman error (10):  $\frac{\partial L(\theta, w)}{\partial w} = \mathbf{0}$ .

**Implicit differentiation.** The process of training  $\theta$  is bi-level: in the inner loop, we optimize the Q-function parameters to get optimal  $w^*$  corresponding to a fixed model  $\theta$ ; in the outer loop, we make a gradient update of  $\theta$ . We make  $K$  steps of an optimization method to approximate  $w^* = \varphi(\theta)$  where  $K$  is a hyperparameter and reuse the weights from the previous outer loop iterations. We follow Rajeswaran et al. [65] and approximate the inverse Jacobian term in  $\frac{\partial \varphi(\theta)}{\partial \theta}$  with the identity matrix. Surprisingly, we did not observe benefits when using the inverse Jacobian term. We investigate the phenomenon deeper and discuss possible explanations in Appendix C.

**Objective.** We consider the problem (6) and use the Bellman error as the outer loop objective:

$$L^{\text{true}}(w) \triangleq \mathbb{E}_{s,a}[Q_w(s, a) - BQ_{\bar{w}}(s, a)]^2, \quad (11)$$

where  $B$ , again, is the soft Bellman optimality operator induced by the true reward  $r$  and dynamics  $p$ .

Note that the objective (11) is used for estimating the gradient with respect to  $\theta$  *only* and  $w$  is trained to optimize  $L(\theta, w)$ . While both  $L^{\text{true}}$  and  $J$  objectives could be used for training  $\theta$ , we found that the latter requires more samples to converge. Note that optimizing the  $L^{\text{true}}$  still corresponds to maximizing the (entropy-regularized) expected returns.

**Resulting gradient.** The changes above in the objective function and the constraint yield the following optimization problem:

$$\min_{w, \theta} L^{\text{true}}(w) \quad \text{s.t.} \quad \frac{\partial L(\theta, w)}{\partial w} = \mathbf{0}. \quad (12)$$

The Q-function and IFT approximations and result in the following gradient with respect to the model parameters:

$$\frac{\partial L^{\text{true}}(\theta)}{\partial \theta} \approx - \underbrace{\frac{\partial L^{\text{true}}(w^*)}{\partial w}}_{\text{grad Bellman}} \cdot \underbrace{\frac{\partial^2 L(\theta, w^*)}{\partial \theta \partial w}}_{\text{approx IFT}} \Big|_{w^* = \varphi(\theta)} \quad (13)$$

The OMD algorithm is summarised in Algorithm 1. The only difference between Dyna-based approaches and OMD (highlighted in blue) is given by the gradient used to train model parameters  $\theta$ .

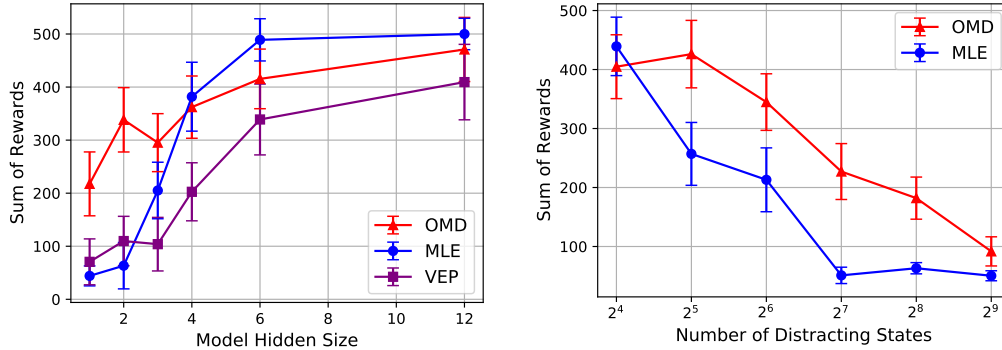


Figure 4: **Left:** The final performance of the agents in CartPole for varying hidden dimensionality of the model networks. The OMD model makes useful predictions under the model misspecification. **Right:** The performance when the state space is augmented with uninformative noise. OMD is more robust as the number of distractor increases, while VEP fails for any positive number of distractors. The error bar is the standard error measured over 10 random seeds.

## 7 Experiments with Function Approximation

This section aims to test the following hypotheses:

- The OMD agent with approximations from Section 6 achieves near-optimal returns.
- The performance of OMD is better compared to MLE under the model misspecification.
- The parameters  $\theta$  of the OMD model have low likelihood, yet the agent that acts using the Q-function trained with the model achieves near-optimal returns in the true MDP.

**Setup.** We provide full details about the experimental setup and hyperparameters in Appendix D. We choose CartPole [9] to have controllable experiments but also include results on MuJoCo HalfCheetah [78] with similar findings in Appendix F further supporting our conclusions. Since OMD learns one of the  $Q^*$ -equivalent models as shown in Section 5.1, a close non-MLE baseline would be the algorithm used in the value equivalence principle (VEP) paper [30]. The VEP model minimizes the difference between the Bellman operators:

$$\ell_{\text{VEP}}(\theta) = \sum_{\pi \in \Pi} \sum_{V \in \mathcal{V}} \sum_{s \in \mathcal{S}} (B_{\pi} V(s) - B_{\pi}^{\theta} V(s))^2, \quad (14)$$

where  $B_{\pi}^{\theta} V(s) = \mathbb{E}_{a \sim \pi(a|s), s' \sim p_{\theta}(s'|s,a)} (r_{\theta}(s,a) + \gamma V(s'))$ ,  $B_{\pi}$  is the real model counterpart estimated from samples, and  $\Pi$  and  $\mathcal{V}$  are predefined sets of policies and value functions.

**Performance under model misspecification.** We design two experiments that allow measuring the misspecification in isolation. First, we limit the model class representational capacity by controlling the number of units in hidden layers of the model. Next, we add distracting states by sampling noise from a standard gaussian and vary the number of distractors. Figure 4 shows the returns achieved by the agents after training in the two regimes. Note that the Q-function is updated using only the next states and rewards produced by the model, and even when the hidden dimensionality of the model is 1, the OMD model encodes useful information for taking optimal actions. Returns achieved by OMD are also more robust to the distractors indicating that the MLE focuses on predicting the parts of a state that might not be relevant for decision making. The relatively poor performance of VEP suggests that learning a model to predict values for a fixed set of policies and value functions is not as effective, especially if some states are non-informative. The experiments reflect the challenges an MBRL agent will face in complex domains such as [11, 10, 45]: accurately predicting the next observations can be infeasible because the underlying dynamics can be too involved and there might be few components that are important for taking action. Figure 4 provides evidence that using control-oriented methods would allow using the model capacity more effectively.

**Likelihood of OMD model.** We show the mean squared error (MSE) of OMD and MLE dynamics predictions in Figure 5. Quantitatively, the MSE of OMD models is *higher than the MSE of a randomly initialized model*, while OMD achieves higher returns than MLE. This finding suggests that the dynamics might not need to produce predictions close to the true states to be useful for planning.

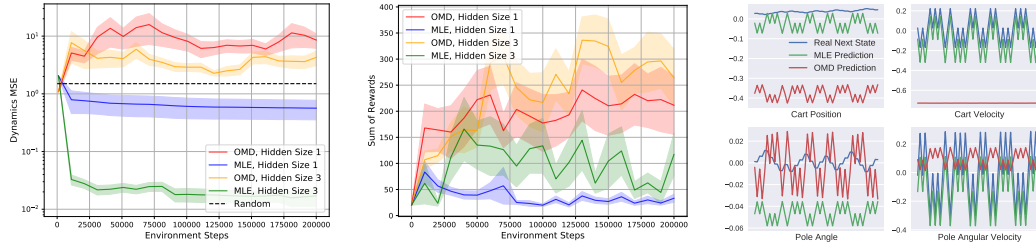


Figure 5: **Left:** Mean squared error (MSE) of the next state prediction of OMD and MLE models in CartPole under model misspecification (number of hidden units 1 and 3). The shaded region is the standard error over 10 runs. **Center:** The corresponding returns of OMD and MLE agents. OMD returns are larger than the returns of MLE even though MLE predicts the next states more accurately. **Right:** Next state predictions of OMD and MLE models with hidden size 1. The OMD agent discards Cart Velocity and predicts unrealistic Cart Position but achieves the optimal returns of 500.

Qualitatively, we visualize individual coordinates of the predictions under the model misspecification in Figure 5. We predict the immediate next states given a sequence of states and actions from an optimal trajectory. We use one of the runs of the OMD agent with the hidden size 1 that achieves optimal returns of 500 and observe that Cart Velocity predictions are nearly constant. On the other hand, an MLE model with the hidden size 1 spends its limited capacity to predict the fluctuations in Cart Velocity leading to a significant deterioration in obtained returns.

Overall, these findings suggest that the OMD agent achieves near-optimal returns, performs better than the MLE-based MBRL agent as well as VEP under model misspecification, and learns a model that is useful for control despite having low likelihood.

## 8 Discussion and Future Work

An exciting direction for future work is the extension of OMD to environments with image-based observations where model misspecification naturally arises. We expect that for complex visual domains, learning a control-oriented model should be more effective compared to model-based methods that rely on reconstruction [44, 34]. Based on Figure 5, we also conjecture that OMD can learn an abstract model that can ignore parts of the original state space that are irrelevant for control. This might allow applying OMD in a zero-shot manner for transfer learning tasks where the underlying dynamics remain unchanged.

Implicit differentiation is not the only way to solve the described constrained optimization problems. Other alternatives include using Lagrangian methods as proposed for the tabular case in [7]. Since extending the approach to non-tabular MDPs would require an additional approximator for Lagrange multipliers, we conjecture that finding a saddle point is going to be less stable than using the IFT.

Finally, it is worth theoretically studying the sensitivity of the IFT to the approximations to the inverse Jacobian term and the inner loop solutions. Our findings, as well as findings of [64, 65, 54] suggest that there is a gap between the assumptions of the IFT and its applicability in practice.

## 9 Conclusion

The paper proposes *optimal model design* (OMD), a method for learning control-oriented models that addresses the shortcomings of likelihood-based MBRL approaches. OMD optimizes the expected returns in an end-to-end manner and alleviates the objective mismatch of standard MBRL methods that train models using a proxy of the true RL objective. Theoretically, we characterize the set of optimal solutions to OMD and illustrate the efficacy of OMD over MLE agents for approximating optimal value functions. Empirically, we introduce approximations to apply OMD to non-tabular environments and demonstrate the improved performance of OMD in settings with limited model capacity. Perhaps surprisingly, we find that the OMD model can have low likelihood, yet the model is useful for maximizing returns. Overall, OMD sheds light on the potential of control-oriented models for model-based reinforcement learning.

## Acknowledgments and Disclosure of Funding

EN thanks Iurii Kemaev and Clement Gehring for invaluable help with JAX; Tristan Deleu, Gauthier Gidel, Amy Zhang, Aravind Rajeswaran, Ilya Kostrikov, Brandon Amos, and Aaron Courville for insightful discussions; Pierluca D’Oro, David Brandfonbrener, Valentin Thomas, and Timur Garipov for useful suggestions on the early draft of the paper; Compute Canada for providing computational resources. This work was partially supported by Facebook CIFAR AI Chair and IVADO.

We acknowledge the Python community [80, 63] for developing the core set of tools that enabled this work, including JAX [15], Jupyter [47], Matplotlib [38], numpy [62, 79], pandas [58], and SciPy [42].

## References

- [1] Romina Abachi, Mohammad Ghavamzadeh, and Amir-massoud Farahmand. Policy-aware model learning for policy gradient methods. *arXiv preprint arXiv:2003.00030*, 2020.
- [2] M. Abbad and J.A. Filar. Perturbation and stability theory for markov control problems. *IEEE Transactions on Automatic Control*, 37(9):1415–1420, 1992. doi: 10.1109/9.159584.
- [3] Brandon Amos and Denis Yarats. The differentiable cross-entropy method. In *International Conference on Machine Learning*, pages 291–302. PMLR, 2020.
- [4] Brandon Amos, Ivan Jimenez, Jacob Sacks, Byron Boots, and J Zico Kolter. Differentiable mpc for end-to-end planning and control. In *Advances in Neural Information Processing Systems*, pages 8289–8300, 2018.
- [5] Alex Ayoub, Zeyu Jia, Csaba Szepesvari, Mengdi Wang, and Lin F Yang. Model-based reinforcement learning with value-targeted regression. *arXiv preprint arXiv:2006.01107*, 2020.
- [6] Igor Babuschkin, Kate Baumli, Alison Bell, Surya Bhupatiraju, Jake Bruce, Peter Buchlovsky, David Budden, Trevor Cai, Aidan Clark, Ivo Danihelka, Claudio Fantacci, Jonathan Godwin, Chris Jones, Tom Hennigan, Matteo Hessel, Steven Kapturowski, Thomas Keck, Iurii Kemaev, Michael King, Lena Martens, Vladimir Mikulik, Tamara Norman, John Quan, George Papanikaros, Roman Ring, Francisco Ruiz, Alvaro Sanchez, Rosalia Schneider, Eren Sezener, Stephen Spencer, Srivatsan Srinivasan, Wojciech Stokowiec, and Fabio Viola. The DeepMind JAX Ecosystem, 2020. URL <http://github.com/deepmind>.
- [7] Pierre-Luc Bacon, Florian Schäfer, Clement Gehring, Animashree Anandkumar, and Emma Brunskill. A lagrangian method for inverse problems in reinforcement learning. In *Optimization in RL workshop at NeurIPS 2019*, 2019.
- [8] Shaojie Bai, J Zico Kolter, and Vladlen Koltun. Deep equilibrium models. In *Advances in Neural Information Processing Systems*, pages 690–701, 2019.
- [9] Andrew G Barto, Richard S Sutton, and Charles W Anderson. Neuronlike adaptive elements that can solve difficult learning control problems. *IEEE transactions on systems, man, and cybernetics*, (5):834–846, 1983.
- [10] Charles Beattie, Joel Z Leibo, Denis Teplyashin, Tom Ward, Marcus Wainwright, Heinrich Küttler, Andrew Lefrancq, Simon Green, Víctor Valdés, Amir Sadik, et al. Deepmind lab. *arXiv preprint arXiv:1612.03801*, 2016.
- [11] Marc G Bellemare, Yavar Naddaf, Joel Veness, and Michael Bowling. The arcade learning environment: An evaluation platform for general agents. *Journal of Artificial Intelligence Research*, 47:253–279, 2013.
- [12] Byron Boots, Sajid M. Siddiqi, and Geoffrey J. Gordon. Closing the learning-planning loop with predictive state representations. *Int. J. Robotics Res.*, 30(7):954–966, 2011. doi: 10.1177/0278364911404092.
- [13] V. Borkar and P. Varaiya. Adaptive control of markov chains, i: Finite parameter set. *IEEE Transactions on Automatic Control*, 24(6):953–957, December 1979.

- [14] Stephen Boyd, Stephen P Boyd, and Lieven Vandenberghe. *Convex optimization*. Cambridge university press, 2004.
- [15] James Bradbury, Roy Frostig, Peter Hawkins, Matthew James Johnson, Chris Leary, Dougal Maclaurin, George Necula, Adam Paszke, Jake VanderPlas, Skye Wanderman-Milne, and Qiao Zhang. JAX: composable transformations of Python+NumPy programs, 2018. URL <http://github.com/google/jax>.
- [16] Bruce Christianson. Reverse accumulation and attractive fixed points. *Optimization Methods and Software*, 3(4):311–326, January 1994. doi: 10.1080/10556789408805572.
- [17] Kurtland Chua, Roberto Calandra, Rowan McAllister, and Sergey Levine. Deep reinforcement learning in a handful of trials using probabilistic dynamics models. In *Advances in Neural Information Processing Systems*, pages 4754–4765, 2018.
- [18] Robert Dadashi, Adrien Ali Taiga, Nicolas Le Roux, Dale Schuurmans, and Marc G Bellemare. The value function polytope in reinforcement learning. In *International Conference on Machine Learning*, pages 1486–1495. PMLR, 2019.
- [19] Yann Dauphin, Razvan Pascanu, Caglar Gulcehre, Kyunghyun Cho, Surya Ganguli, and Yoshua Bengio. Identifying and attacking the saddle point problem in high-dimensional non-convex optimization. *arXiv preprint arXiv:1406.2572*, 2014.
- [20] Eric V. Denardo. Contraction mappings in the theory underlying dynamic programming. *SIAM Review*, 9(2):165–177, April 1967. doi: 10.1137/1009030.
- [21] Peter Dorato, Vito Cerone, and Chaouki Abdallah. *Linear-quadratic control: an introduction*. Simon & Schuster, Inc., 1994.
- [22] Pierluca D’Oro, Alberto Maria Metelli, Andrea Tirinzoni, Matteo Papini, and Marcello Restelli. Gradient-aware model-based policy search. In *Proceedings of the AAAI Conference on Artificial Intelligence*, volume 34, pages 3801–3808, 2020.
- [23] Amir-massoud Farahmand, Andre Barreto, and Daniel Nikovski. Value-aware loss function for model-based reinforcement learning. In *Artificial Intelligence and Statistics*, pages 1486–1494, 2017.
- [24] Chelsea Finn, Pieter Abbeel, and Sergey Levine. Model-agnostic meta-learning for fast adaptation of deep networks. In *International Conference on Machine Learning*, pages 1126–1135. PMLR, 2017.
- [25] Scott Fujimoto, Herke Hoof, and David Meger. Addressing function approximation error in actor-critic methods. In *International Conference on Machine Learning*, pages 1587–1596. PMLR, 2018.
- [26] Clement Gehring, Pierre-Luc Bacon, and Florian Schaefer. FAX: differentiating fixed point problems in JAX, 2019. Available at: <https://github.com/gehring/fax>.
- [27] J. P. Georgin. Estimation et controle des chaines de markov sur des espaces arbitraires. In *Lecture Notes in Mathematics*, pages 71–113. Springer Berlin Heidelberg, 1978. doi: 10.1007/bfb0063261.
- [28] John J. Grefenstette, Connie Loggia Ramsey, and Alan C. Schultz. Learning sequential decision rules using simulation models and competition. *Machine Learning*, 5(4):355–381, October 1990. doi: 10.1007/bf00116876.
- [29] Andreas Griewank and Andrea Walther. *Evaluating Derivatives*. Society for Industrial and Applied Mathematics, January 2008.
- [30] Christopher Grimm, André Barreto, Satinder Singh, and David Silver. The value equivalence principle for model-based reinforcement learning. *Advances in Neural Information Processing Systems*, 33, 2020.

- [31] Tuomas Haarnoja, Aurick Zhou, Pieter Abbeel, and Sergey Levine. Soft actor-critic: Off-policy maximum entropy deep reinforcement learning with a stochastic actor. In *International Conference on Machine Learning*, pages 1861–1870. PMLR, 2018.
- [32] Tuomas Haarnoja, Aurick Zhou, Kristian Hartikainen, George Tucker, Sehoon Ha, Jie Tan, Vikash Kumar, Henry Zhu, Abhishek Gupta, Pieter Abbeel, et al. Soft actor-critic algorithms and applications. *arXiv preprint arXiv:1812.05905*, 2018.
- [33] Danijar Hafner, Timothy Lillicrap, Ian Fischer, Ruben Villegas, David Ha, Honglak Lee, and James Davidson. Learning latent dynamics for planning from pixels. In *International Conference on Machine Learning*, pages 2555–2565. PMLR, 2019.
- [34] Danijar Hafner, Timothy Lillicrap, Mohammad Norouzi, and Jimmy Ba. Mastering atari with discrete world models. *arXiv preprint arXiv:2010.02193*, 2020.
- [35] Hado Hasselt. Double q-learning. *Advances in neural information processing systems*, 23: 2613–2621, 2010.
- [36] Jonathan Heek, Anselm Levskaya, Avital Oliver, Marvin Ritter, Bertrand Rondepierre, Andreas Steiner, and Marc van Zee. Flax: A neural network library and ecosystem for JAX, 2020. URL <http://github.com/google/flax>.
- [37] O. Hernández-Lerma and S. I. Marcus. Adaptive control of discounted markov decision chains. *Journal of Optimization Theory and Applications*, 46(2):227–235, June 1985. doi: 10.1007/bf00938426.
- [38] John D Hunter. Matplotlib: A 2d graphics environment. *IEEE Annals of the History of Computing*, 9(03):90–95, 2007.
- [39] Garud N. Iyengar. Robust dynamic programming. *Mathematics of Operations Research*, 30(2): 257–280, May 2005. doi: 10.1287/moor.1040.0129.
- [40] Michael Janner, Justin Fu, Marvin Zhang, and Sergey Levine. When to trust your model: Model-based policy optimization. In *Advances in Neural Information Processing Systems*, pages 12519–12530, 2019.
- [41] Nan Jiang. Lecture notes on statistical reinforcement learning. 2018.
- [42] Eric Jones, Travis Oliphant, and Pearu Peterson. *SciPy: Open source scientific tools for Python*. 2014.
- [43] Joshua Joseph, Alborz Geramifard, John W Roberts, Jonathan P How, and Nicholas Roy. Reinforcement learning with misspecified model classes. In *2013 IEEE International Conference on Robotics and Automation*, pages 939–946. IEEE, 2013.
- [44] Lukasz Kaiser, Mohammad Babaeizadeh, Piotr Milos, Blazej Osinski, Roy H Campbell, Konrad Czechowski, Dumitru Erhan, Chelsea Finn, Piotr Kozakowski, Sergey Levine, et al. Model-based reinforcement learning for atari. *arXiv preprint arXiv:1903.00374*, 2019.
- [45] Dmitry Kalashnikov, Jacob Varley, Yevgen Chebotar, Benjamin Swanson, Rico Jonschkowski, Chelsea Finn, Sergey Levine, and Karol Hausman. Mt-opt: Continuous multi-task robotic reinforcement learning at scale. *arXiv preprint arXiv:2104.08212*, 2021.
- [46] Michael Kearns and Satinder Singh. Near-optimal reinforcement learning in polynomial time. *Machine learning*, 49(2):209–232, 2002.
- [47] Thomas Kluyver, Benjamin Ragan-Kelley, Fernando Pérez, Brian E Granger, Matthias Bussonnier, Jonathan Frederic, Kyle Kelley, Jessica B Hamrick, Jason Grout, Sylvain Corlay, et al. *Jupyter Notebooks-a publishing format for reproducible computational workflows.*, volume 2016. 2016.
- [48] Steven G Krantz and Harold R Parks. *The implicit function theorem: history, theory, and applications*. Springer Science & Business Media, 2012.

- [49] Masami Kurano. Discrete-time markovian decision processes with an unknown parameter-average return criterion. *Journal of the Operations Research Society of Japan*, 15(2):67–76, 1972.
- [50] Nathan Lambert, Brandon Amos, Omry Yadan, and Roberto Calandra. Objective mismatch in model-based reinforcement learning. *arXiv preprint arXiv:2002.04523*, 2020.
- [51] Sergey Levine. Reinforcement learning and control as probabilistic inference: Tutorial and review. *arXiv preprint arXiv:1805.00909*, 2018.
- [52] Lihong Li, Thomas J Walsh, and Michael L Littman. Towards a unified theory of state abstraction for mdps. *ISAIM*, 4:5, 2006.
- [53] Long-Ji Lin. Self-improving reactive agents based on reinforcement learning, planning and teaching. *Machine Learning*, 8(3-4):293–321, May 1992. doi: 10.1007/bf00992699.
- [54] Jonathan Lorraine, Paul Vicol, and David Duvenaud. Optimizing millions of hyperparameters by implicit differentiation. In *International Conference on Artificial Intelligence and Statistics*, pages 1540–1552. PMLR, 2020.
- [55] D. Ludwig and C.J. Walters. Optimal harvesting with imprecise parameter estimates. *Ecological Modelling*, 14(3-4):273–292, January 1982. doi: 10.1016/0304-3800(82)90023-0.
- [56] P. Mandl. Estimation and control in markov chains. *Advances in Applied Probability*, 6(1): 40–60, March 1974. doi: 10.2307/1426206.
- [57] Schäl Manfred. Estimation and control in discounted stochastic dynamic programming. *Stochastics*, 20(1):51–71, January 1987. doi: 10.1080/17442508708833435.
- [58] Wes McKinney. *Python for data analysis: Data wrangling with Pandas, NumPy, and IPython*. "O'Reilly Media, Inc.", 2012.
- [59] Volodymyr Mnih, Koray Kavukcuoglu, David Silver, Andrei A Rusu, Joel Veness, Marc G Bellemare, Alex Graves, Martin Riedmiller, Andreas K Fidjeland, Georg Ostrovski, et al. Human-level control through deep reinforcement learning. *nature*, 518(7540):529–533, 2015.
- [60] Vinod Nair and Geoffrey E Hinton. Rectified linear units improve restricted boltzmann machines. In *Icml*, 2010.
- [61] Arnab Nilim and Laurent El Ghaoui. Robust control of markov decision processes with uncertain transition matrices. *Operations Research*, 53(5):780–798, October 2005. doi: 10.1287/opre.1050.0216.
- [62] Travis E Oliphant. *A guide to NumPy*, volume 1. Trelgol Publishing USA, 2006.
- [63] Travis E Oliphant. Python for scientific computing. *Computing in Science & Engineering*, 9(3): 10–20, 2007.
- [64] Aravind Rajeswaran, Chelsea Finn, Sham M Kakade, and Sergey Levine. Meta-learning with implicit gradients. In *Advances in Neural Information Processing Systems*, pages 113–124, 2019.
- [65] Aravind Rajeswaran, Igor Mordatch, and Vikash Kumar. A game theoretic framework for model based reinforcement learning. *arXiv preprint arXiv:2004.07804*, 2020.
- [66] Reuven Y Rubinstein. Optimization of computer simulation models with rare events. *European Journal of Operational Research*, 99(1):89–112, 1997.
- [67] John Rust. Maximum likelihood estimation of discrete control processes. *SIAM journal on control and optimization*, 26(5):1006–1024, 1988.
- [68] Levent Sagun, Utku Evci, V Ugur Guney, Yann Dauphin, and Leon Bottou. Empirical analysis of the hessian of over-parametrized neural networks. *arXiv preprint arXiv:1706.04454*, 2017.

- [69] M. Sato, K. Abe, and H. Takeda. Learning control of finite markov chains with an explicit trade-off between estimation and control. *IEEE Transactions on Systems, Man, and Cybernetics*, 18(5):677–684, 1988. doi: 10.1109/21.21595.
- [70] Julian Schrittwieser, Ioannis Antonoglou, Thomas Hubert, Karen Simonyan, Laurent Sifre, Simon Schmitt, Arthur Guez, Edward Lockhart, Demis Hassabis, Thore Graepel, et al. Mastering atari, go, chess and shogi by planning with a learned model. *arXiv preprint arXiv:1911.08265*, 2019.
- [71] RE Skelton. Model error concepts in control design. *International Journal of Control*, 49(5): 1725–1753, 1989.
- [72] Jonathan Sorg, Richard L Lewis, and Satinder Singh. Reward design via online gradient ascent. In J. Lafferty, C. Williams, J. Shawe-Taylor, R. Zemel, and A. Culotta, editors, *Advances in Neural Information Processing Systems*, volume 23, pages 2190–2198. Curran Associates, Inc., 2010.
- [73] Richard S Sutton. Dyna, an integrated architecture for learning, planning, and reacting. *ACM Sigart Bulletin*, 2(4):160–163, 1991.
- [74] Richard S Sutton and Andrew G Barto. *Reinforcement learning: An introduction*. MIT press, 2018.
- [75] Richard S Sutton, David McAllester, Satinder Singh, and Yishay Mansour. Policy gradient methods for reinforcement learning with function approximation. *Advances in neural information processing systems*, 12:1057–1063, 1999.
- [76] Aviv Tamar, Yi Wu, Garrett Thomas, Sergey Levine, and Pieter Abbeel. Value iteration networks. *arXiv preprint arXiv:1602.02867*, 2016.
- [77] H. Theil. A note on certainty equivalence in dynamic planning. *Econometrica*, 25(2):346, April 1957.
- [78] Emanuel Todorov, Tom Erez, and Yuval Tassa. Mujoco: A physics engine for model-based control. In *2012 IEEE/RSJ International Conference on Intelligent Robots and Systems*, pages 5026–5033. IEEE, 2012.
- [79] Stefan Van Der Walt, S Chris Colbert, and Gael Varoquaux. The numpy array: a structure for efficient numerical computation. *Computing in science & engineering*, 13(2):22–30, 2011.
- [80] Guido Van Rossum and Fred L Drake Jr. *Python tutorial*, volume 620. Centrum voor Wiskunde en Informatica Amsterdam, 1995.
- [81] Christopher JCH Watkins and Peter Dayan. Q-learning. *Machine learning*, 8(3-4):279–292, 1992.
- [82] Huan Xu and Shie Mannor. Distributionally robust markov decision processes. In J. Lafferty, C. Williams, J. Shawe-Taylor, R. Zemel, and A. Culotta, editors, *Advances in Neural Information Processing Systems*, volume 23, pages 2505–2513. Curran Associates, Inc., 2010.
- [83] Tianhe Yu, Garrett Thomas, Lantao Yu, Stefano Ermon, James Zou, Sergey Levine, Chelsea Finn, and Tengyu Ma. Mopo: Model-based offline policy optimization. In *Advances in Neural Information Processing Systems 33 pre-proceedings*, 2020.
- [84] Brian D Ziebart, Andrew L Maas, J Andrew Bagnell, and Anind K Dey. Maximum entropy inverse reinforcement learning. In *Aaai*, volume 8, pages 1433–1438. Chicago, IL, USA, 2008.

# Supplementary Material

## A Implicit Differentiation in JAX

We provide an implementation of implicit differentiation in JAX [6, 36] by adapting the code from the library for finding fixed points [26]. The implementation requires a *solver* that takes parameters  $\theta$  and an initial  $w_0$  as input and outputs  $\varphi(\theta) = w^*$  such that  $f(\theta, w^*) = 0$ . Then, we define a custom vector-Jacobian product that allows using  $\varphi(\theta)$  as a block in a differentiable computational graph. We highlight the importance of having an implementation *without* explicitly forming the matrices in (7) which is crucial for large-scale applications. The implementation allows using both the version with the inverse Jacobian term as well as with the identity approximation as discussed in Section 6.

```
import jax.numpy as jnp
from jax import custom_vjp, vjp
from functools import partial
from jax.scipy.sparse.linalg import cg

@partial(custom_vjp, nondiff_argnums=(0, 3))
def root_solve(f, w0, p, solver):
    return solver(f, w0, p)

def fwd(f, w0, p, solver):
    sol = root_solve(f, w0, p, solver)
    return sol, (sol, p)

def rev(f, solver, res, g):
    sol, p = res
    _, dp_vjp = vjp(lambda y: f(y, sol), p)
    if USE_IDENTITY_INVERSE:
        vdp = dp_vjp(-g)[0]
    else:
        _, dsol_vjp = vjp(lambda w: f(p, w), sol)
        vdsoli = cg(lambda v: dsol_vjp(v)[0], g)
        vdp = dp_vjp(-vdsoli[0])[0]
    return jnp.zeros_like(sol), vdp

root_solve.defvjp(fwd, rev)
sol = root_solve(f, w0, p, solver)
# solver returns sol: f(p, sol) = 0
# sol is differentiable w.r.t. p
```

The implicit function theorem (IFT), which we prove in the next appendix, allows differentiating outputs of black-box functions  $\varphi(\theta)$  that do not have a closed (differentiable) form. For example, in Section 4.2, function  $\varphi$  takes as input the parameters of the model and applies fixed-point iteration until convergence to find the optimal value function for the given parameters. This contrasts implicit differentiation to other meta-learning algorithms like MAML [24] that differentiate *through* the iterations of the inner loop procedure.

## B Proof of IFT

The implicit function theorem is a well known result discussed in, for example, [48].

**Theorem 1.** (Cauchy, Implicit Function) *Let  $f : \Theta \times \mathcal{W} \rightarrow \mathcal{W}$  be a continuously differentiable function and  $(\tilde{\theta}, \tilde{w})$  be a point satisfying  $f(\tilde{\theta}, \tilde{w}) = \mathbf{0}$ . If the Jacobian  $\frac{\partial f(\tilde{\theta}, \tilde{w})}{\partial w}$  is invertible, then there exists an open set  $U \subseteq \Theta$  containing  $\tilde{\theta}$  and a unique continuously differentiable function  $\varphi$  such that  $\varphi(\tilde{\theta}) = \tilde{w}$  and  $f(\theta, \varphi(\theta)) = \mathbf{0}$  for all  $\theta \in U$ . Moreover,*

$$\frac{\partial \varphi(\theta)}{\partial \theta} = - \left( \frac{\partial f(\theta, w^*)}{\partial w} \right)^{-1} \cdot \frac{\partial f(\theta, w^*)}{\partial \theta} \Big|_{w^* = \varphi(\theta)} \quad \forall \theta \in U. \quad (7)$$

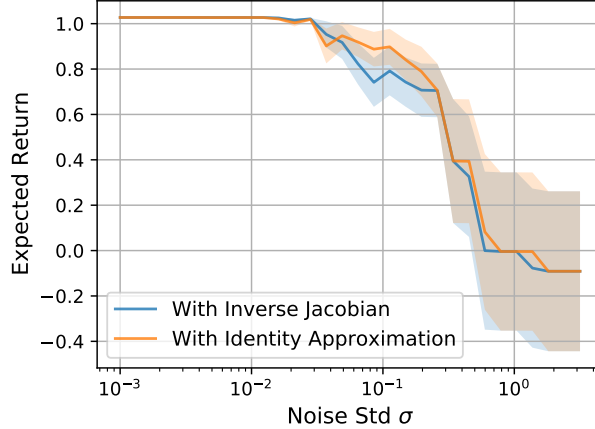


Figure 6: The expected returns as a function of the inner loop solutions noise magnitude  $\sigma$ . OMD with the true and the approximate  $\frac{\partial \varphi(\theta)}{\partial \theta}$  has the same resulting returns as  $\sigma$  increases. The shaded region is the standard error over 10 runs.

*Proof.* By the assumption, we have

$$f(\theta, \varphi(\theta)) = \mathbf{0} \quad \forall \theta \in U.$$

Taking the total derivative of  $f$  with respect to  $\theta$ , we have

$$\frac{\partial f(\theta, w^*)}{\partial \theta} + \frac{\partial f(\theta, w^*)}{\partial w} \frac{\partial \varphi(\theta)}{\partial \theta} \Big|_{w^*=\varphi(\theta)} = \mathbf{0}.$$

Rearranging the terms and using the invertibility of the Jacobian, we get

$$\frac{\partial \varphi(\theta)}{\partial \theta} = - \left( \frac{\partial f(\theta, w^*)}{\partial w} \right)^{-1} \cdot \frac{\partial f(\theta, w^*)}{\partial \theta} \Big|_{w^*=\varphi(\theta)}.$$

□

## C Sensitivity to IFT Approximations

The IFT provides a way to calculate the derivatives of a black-box function  $\varphi$ . The expression (7) is valid under the assumptions that

1. the inner loop solution  $w^*$  satisfies the equation  $f(\theta, w^*) = 0$  exactly;
2. the Jacobian term  $\frac{\partial f(\theta, w^*)}{\partial w}$  is inverted accurately.

Ensuring both of the conditions can be challenging for large-scale applications. This appendix analyzes the sensitivity to the conditions in a controlled manner for the 2-state MDP from Figure 3, while Appendix E studies the sensitivity for the function approximation case. At every outer loop iteration, we calculate the exact  $w^*$ , add gaussian noise with standard deviation  $\sigma$ , and observe the effect on the expected returns  $J$  after the convergence of  $\theta$ . Figure 6 demonstrates the results for the exact outer loop gradient  $\frac{\partial \varphi(\theta)}{\partial \theta}$  as well as the gradient using the identity approximation of the inverse Jacobian term. Surprisingly, we did not observe significant benefits of using the Jacobian  $\frac{\partial f(\theta, w^*)}{\partial w}$ . We conjecture that the inverse Jacobian acts like a preconditioner [14] on  $\frac{\partial \varphi(\theta)}{\partial \theta}$  and the preconditioner is useful in our setting only near the exact inner loop solutions  $w^*$ . We leave the theoretical investigation of the IFT sensitivity as future work and refer the reader to Lorraine et al. [54] for a discussion about approximations of the Jacobian term.

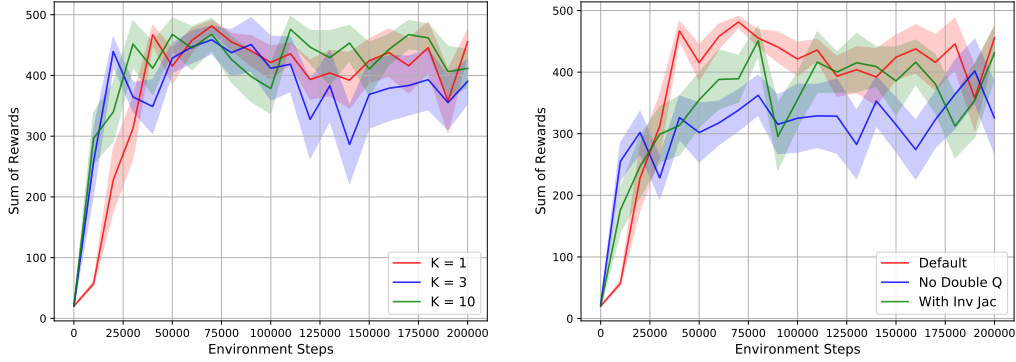


Figure 7: **Left:** Returns of OMD agents for the varying number of inner loop steps  $K$  per outer loop step. The difference between 1, 3, and 10 steps is insignificant. **Right:** The evaluation returns of OMD agents for the default agent, the agent without double Q learning, and the agent without the identity approximation of the inverse Jacobian. Using two Q networks increases the returns while using the inverse Jacobian does not change the performance significantly. The shaded region is the standard error over 10 runs.

## D Experimental Details

In Section 7, we use CartPole [9], an environment with 2 actions, 4-dimensional continuous state space, and optimal returns of 500. We train the agents for 200000 environment steps. The temperature  $\alpha$  is 0.01. We sample from the replay buffer with a mini-batch size of 256. The discount factor  $\gamma$  is 0.99. At each time step during training, the agent chooses a random action with a probability of 0.1 for exploration. We have a separate copy of the environment where we evaluate the agent and take the average over 10 runs to estimate the returns. We run each experiment using 10 random seeds.

We set the number of Q-function updates  $K$  equal to 1. For the results with  $K = 3$  and  $K = 10$ , see Figure 7. We highlight that after each outer loop step, weights  $w$  are warm-started using the last iterate of the previous inner loop (instead of randomly initializing  $w$  and training from scratch). We use Adam optimizer with the learning rate  $10^{-3}$  for updating  $\theta$  and perform a hyperparameter sweep over the learning rate for  $w$  in  $\{3 \cdot 10^{-4}, 10^{-3}, 3 \cdot 10^{-3}\}$ . We make a sweep over the moving average coefficient  $\tau$  for the target network  $\bar{w}$  in  $\{0.005, 0.01\}$ . Both of the parameters control how fast the Q-network parameters are updated relatively to the model parameters. Since the CartPole environment is non-stochastic, we use a deterministic dynamics model. All networks have two hidden layers and ReLU activations [60]. For both hidden layers in all networks, we set the dimensionality to 32. In the experiment with the limited model class capacity, we vary the hidden dimensionality in  $\{1, 2, 3, 4, 6, 12\}$  for the dynamics and reward networks to measure how the limitation affects the agent’s performance. In the experiment with the distractors, we vary the number of gaussians in  $\{2^4, 2^5, 2^6, 2^7, 2^8, 2^9\}$  to measure how the uninformative state components affect the returns.

For the value equivalence principle (VEP) baseline, we have followed the experimental setup from the original paper [30]. Perhaps surprisingly, the authors find that it suffices to use a set of all deterministic state-independent policies as  $\Pi$  and 5 random value functions as  $\mathcal{V}$  for CartPole (see Appendix A.2.3 in [30]).

We have used CPU-only nodes of the internal cluster. Each experiment requires  $10 \text{ seeds} \times 3 \text{ algorithms} \times 2 \text{ } \tau \text{'s} \times 6 \text{ hidden sizes} / 6 \text{ numbers of distractors} \times 3 \text{ LR's}$  resulting in 2160 total jobs.

## E Ablation Study

Section 6 introduces a series of approximations to scale the OMD algorithm to non-tabular environments. We analyze the effect of the approximations by varying the number of inner loop steps  $K$ , using the inverse Jacobian term, and using a single Q-function estimator (without double Q-learning). Figure 7 summarizes the findings of the ablations. We did not observe significant changes in performance for different values of  $K$  for CartPole. The result suggests that as long as the Q-network

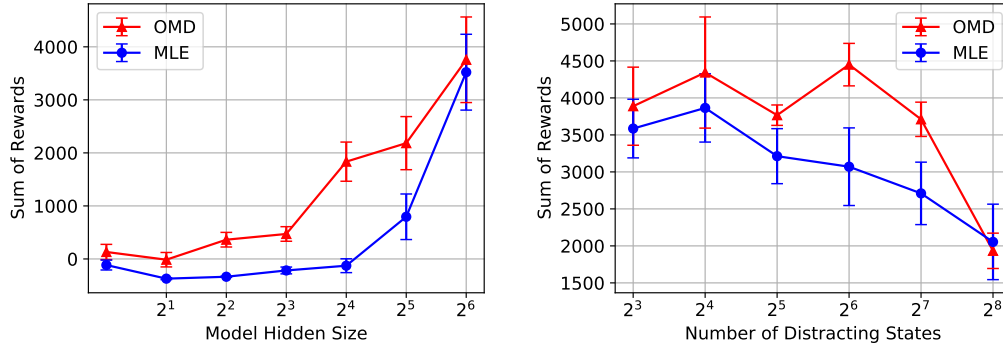


Figure 8: Comparison of OMD and MLE under the model misspecification on HalfCheetah-v2. **Left:** Returns for varying representational capacity of the model. **Right:** Returns when the state space is augmented with uninformative noise. In both settings, the OMD model makes more useful predictions. The std is measured over 5 runs.

update speed (which is also controlled by the target update coefficient  $\tau$  and learning rates) stays aligned with the model update speed, adding more inner loop steps is not necessary.

We observed that Q-functions trained with OMD can be prone to overestimation of Q-values showing that double Q-learning is important for OMD. We conjecture that training a model that maximizes the returns can amplify the overestimation bias [35] caused by using (soft) maximized sampled targets.

Surprisingly, we did not observe significant benefits from using the inverse Jacobian  $\left(\frac{\partial f(\theta, w^*)}{\partial w}\right)^{-1}$ .

We conjecture that there are two reasons explaining the phenomenon. First, the modified constraint in (12) forces the gradient of  $L(\theta, w)$  to be zero, implying that the Jacobian is in fact the Hessian matrix  $\frac{\partial^2 L(\theta, w^*)}{\partial w^2}$ . Dauphin et al. [19], Sagun et al. [68] observed that Hessians of neural networks tend to be singular. Since a system of linear equations with a singular matrix has multiple solutions, it is up to a linear algebra solver to choose the solution. One of the alternatives would be a min-norm solution corresponding to the Moore-Penrose pseudoinverse and the solution might not be providing a useful inductive bias for the learning process of  $\theta$ . Second, the Jacobian term could be useful only in proximity to the exact inner loop solution  $w^*$ . Since the practical algorithm performs only  $K$  inner loop steps and does not reach the exact  $w^*$ , the curvature information provided by the Jacobian might not be beneficial for training  $\theta$ .

Finally, we tried to use the gradient constraint in (12) in the tabular setting. We got similar results as with the constraint on Q-values in (2) suggesting that the two constraints have similar effects on the learning process. Overall, the ablation study provides evidence that OMD is robust to the choice of the number of inner loop steps and the IFT approximations, while double Q-learning is the only important algorithmic modification.

## F Results on HalfCheetah

We provide an additional comparison of OMD and MLE agents under the model misspecification on MuJoCo HalfCheetah [78]. For both agents, the inner optimizer is Soft Actor-Critic (SAC) [31, 32] with the default configuration. OMD trains the model using 13. The MLE agent trains the model with MSE effectively becoming the MBPO algorithm [40] without having an ensemble of models and learning the variance of the predictions.

We perform a hyperparameter sweep over the model learning rate in  $\{10^{-4}, 3 \cdot 10^{-4}\}$ , over the SAC networks learning rate in  $\{10^{-4}, 3 \cdot 10^{-4}\}$ , and over  $K$  in  $\{1, 3\}$ . Model hidden size is 64 for the experiment with distractors.

Figure 8 summarizes the results. Similarly to the observations on the tabular and CartPole environments, the experiments provide evidence that OMD should be preferred over the likelihood-based agent in the model misspecification setup.

## G Proof of Bounds

Section 5.2 discusses the bounds on  $Q^*$  approximation error obtained by the MLE and OMD agents. We first prove a lemma relating the error of the model approximation and the Bellman operator approximation. We then prove a theorem giving a bound on  $Q^*$  error. For simplicity, we focus on the case with the Bellman error in the true MDP (6) as the objective function and “hard” versions of the Bellman optimality operators which are obtained by taking the limit of the log-sum-exp temperature  $\alpha \rightarrow 0$ . Note that results for MLE hold for any agent that approximates the reward and dynamics functions, but we call the agent MLE since it is a common choice for model parameters estimation.

**Notation.** We denote  $p(\cdot|s, a)$  and  $Q(\cdot, a)$  as vectors of transition probabilities and Q-values for all states in  $\mathcal{S}$ . The MLE model is given by  $(\hat{p}, \hat{r})$  and the corresponding Bellman optimality operator is denoted as  $\hat{B}Q$ . To have a distinction between OMD and MLE, we denote OMD parameters as  $\hat{\theta}$  and the corresponding operator as  $B^{\hat{\theta}}Q$ .  $\|f\|_\infty = \sup_x |f(x)|$  is the infinity norm of a function  $f$ .  $\mathbf{1}$  is a vector of an appropriate size with ones as entries.

**Lemma 1.** (Bellman operator error bound) *Let  $Q$  be an action-value function. If the dynamics  $\hat{p}$  and the reward  $\hat{r}$  have the bounded errors  $\max_{s,a} \|p(\cdot|s, a) - \hat{p}(\cdot|s, a)\|_1 = \epsilon_p$  and  $\max_{s,a} |r(s, a) - \hat{r}(s, a)| = \epsilon_r$ , and the reward function is bounded  $r(s, a) \in [0, r_{\max}] \forall s, a$ , we have*

$$\|BQ - \hat{B}Q\|_\infty \leq \epsilon_r + \frac{\gamma \epsilon_p r_{\max}}{2(1-\gamma)}. \quad (15)$$

*Proof.* Using the derivations similar to the proof of the simulation lemma [41], we obtain for any state-action pair  $(s, a)$

$$\begin{aligned} & \left| BQ(s, a) - \hat{B}Q(s, a) \right| \\ &= \left| \left( r(s, a) + \gamma \sum_{s'} p(s'|s, a) \max_{a'} Q(s', a') \right) - \left( \hat{r}(s, a) + \gamma \sum_{s'} \hat{p}(s'|s, a) \max_{a'} Q(s', a') \right) \right| \\ &\leq |r(s, a) - \hat{r}(s, a)| + \gamma \left| \sum_{s'} (p(s'|s, a) - \hat{p}(s'|s, a)) \max_{a'} Q(s', a') \right| \\ &\leq \epsilon_r + \gamma \left| \sum_{s'} (p(s'|s, a) - \hat{p}(s'|s, a)) \left( \max_{a'} Q(s', a') - \frac{r_{\max}}{2(1-\gamma)} \right) \right| \quad \because p \text{ and } \hat{p} \text{ are distributions} \\ &\leq \epsilon_r + \gamma \|p(\cdot|s, a) - \hat{p}(\cdot|s, a)\|_1 \cdot \left\| \max_{a'} Q(\cdot, a') - \frac{r_{\max}}{2(1-\gamma)} \mathbf{1} \right\|_\infty \quad \because \text{H\"older's inequality} \\ &\leq \epsilon_r + \gamma \epsilon_p \left\| \max_{a'} Q(\cdot, a') - \frac{r_{\max}}{2(1-\gamma)} \mathbf{1} \right\|_\infty \\ &\leq \epsilon_r + \frac{\gamma \epsilon_p r_{\max}}{2(1-\gamma)} \quad \because 0 \leq Q(s', a') \leq \frac{r_{\max}}{1-\gamma}. \end{aligned}$$

Since the inequalities hold for all state-action pairs, we can take the maximum over  $(s, a)$  and obtain

$$\max_{s,a} \left| BQ(s, a) - \hat{B}Q(s, a) \right| \leq \epsilon_r + \frac{\gamma \epsilon_p r_{\max}}{2(1-\gamma)}.$$

□

**Theorem 2.** ( $Q^*$  approximation error) *Let  $Q^*$  be the optimal action-value function for the true MDP. Let  $\hat{Q}_{\text{OMD}}$  and  $\hat{Q}_{\text{MLE}}$  be the fixed points of the Bellman optimality operators for approximate OMD and MLE models respectively. Then,*

- *If the MLE dynamics  $\hat{p}$  and reward  $\hat{r}$  have the bounded errors  $\max_{s,a} \|p(\cdot|s, a) - \hat{p}(\cdot|s, a)\|_1 = \epsilon_p$  and  $\max_{s,a} |r(s, a) - \hat{r}(s, a)| = \epsilon_r$ , and the reward function is bounded  $r(s, a) \in [0, r_{\max}] \forall s, a$ , we have*

$$\max_{s,a} \left| Q^*(s, a) - \hat{Q}_{\text{MLE}}(s, a) \right| \leq \frac{\epsilon_r}{1-\gamma} + \frac{\gamma \epsilon_p r_{\max}}{2(1-\gamma)^2};$$

- If the Bellman optimality operator induced by the OMD model  $\hat{\theta}$  has the bounded error  $\max_{s,a} |B\hat{Q}_{\text{OMD}}(s,a) - B^{\hat{\theta}}\hat{Q}_{\text{OMD}}(s,a)| = \epsilon$ , we have

$$\max_{s,a} |Q^*(s,a) - \hat{Q}_{\text{OMD}}(s,a)| \leq \frac{\epsilon}{1-\gamma}.$$

*Proof. (OMD)* For all state-action pairs  $(s, a)$  we get

$$\begin{aligned} & |Q^*(s,a) - \hat{Q}(s,a)| \\ = & |BQ^*(s,a) - B^{\hat{\theta}}\hat{Q}(s,a)| \quad \because \text{Fixed point} \\ = & |BQ^*(s,a) - B\hat{Q}(s,a) + B\hat{Q}(s,a) - B^{\hat{\theta}}\hat{Q}(s,a)| \\ \leq & |BQ^*(s,a) - B\hat{Q}(s,a)| + |B\hat{Q}(s,a) - B^{\hat{\theta}}\hat{Q}(s,a)| \\ \leq & \epsilon + |BQ^*(s,a) - B\hat{Q}(s,a)| \\ = & \epsilon + \left| \left( r(s,a) + \gamma \sum_{s'} p(s'|s,a) \max_{a'} Q^*(s',a') \right) - \left( r(s,a) + \gamma \sum_{s'} p(s'|s,a) \max_{a'} \hat{Q}(s',a') \right) \right| \\ = & \epsilon + \gamma \left| \sum_{s'} p(s'|s,a) \left( \max_{a'} Q^*(s',a') - \max_{a'} \hat{Q}(s',a') \right) \right| \\ \leq & \epsilon + \gamma \|p(\cdot|s,a)\|_1 \cdot \left\| \max_{a'} Q^*(\cdot, a') - \max_{a'} \hat{Q}(\cdot, a') \right\|_{\infty} \quad \because \text{H\"older's inequality} \\ = & \epsilon + \gamma \left\| \max_{a'} Q^*(\cdot, a') - \max_{a'} \hat{Q}(\cdot, a') \right\|_{\infty} \quad \because p \text{ is a distribution} \\ \leq & \epsilon + \gamma \max_{a'} \left\| Q^*(\cdot, a') - \hat{Q}(\cdot, a') \right\|_{\infty} \\ = & \epsilon + \gamma \max_{s',a'} |Q^*(s',a') - \hat{Q}(s',a')|. \end{aligned}$$

Taking the maximum over  $(s, a)$ , we get the recursion:

$$\begin{aligned} \max_{s,a} |Q^*(s,a) - \hat{Q}(s,a)| & \leq \epsilon + \gamma \max_{s,a} |Q^*(s,a) - \hat{Q}(s,a)| \\ \max_{s,a} |Q^*(s,a) - \hat{Q}(s,a)| & \leq \frac{\epsilon}{(1-\gamma)}. \end{aligned}$$

**(MLE)** The proof for MLE can be obtained using the same derivations and additionally using the result of the lemma bounding the difference between the Bellman operators:

$$\epsilon = \max_{s,a} |B\hat{Q}_{\text{MLE}}(s,a) - \hat{B}\hat{Q}_{\text{MLE}}(s,a)| \leq \epsilon_r + \frac{\gamma\epsilon_p r_{\max}}{2(1-\gamma)}.$$

□

The last inequality demonstrates that the OMD bound is tighter. OMD model directly optimizes  $|B\hat{Q}(s,a) - \hat{Q}(s,a)| = |B\hat{Q}(s,a) - B^{\hat{\theta}}\hat{Q}(s,a)|$ , while MLE minimizes  $\epsilon_r$  and  $\epsilon_p$  that only upper bound  $|B\hat{Q}(s,a) - \hat{B}\hat{Q}(s,a)|$  as suggested by the lemma. Hence, given the same budget of representational capacity, OMD will learn a model that is more helpful for approximating the optimal Q-function. Finally, Figure 3 empirically supports our theoretical findings showing that both the  $Q^*$  approximation error and the error-bound gap are smaller for OMD.